

Discovery of Molecular Hydrogen in White Dwarf Atmospheres

S. Xu(许偲艺)^a, M. Jura^a, D. Koester^b, B. Klein^a, B. Zuckerman^a

ABSTRACT

With the Cosmic Origins Spectrograph onboard the *Hubble Space Telescope*, we have detected molecular hydrogen in the atmospheres of three white dwarfs with effective temperatures below 14,000 K, G29-38, GD 133 and GD 31. This discovery provides new independent constraints on the stellar temperature and surface gravity of white dwarfs.

Subject headings: white dwarfs, atmospheres

1. INTRODUCTION

An important discovery from the *International Ultraviolet Explorer (IUE)* was two broad absorption features at 1400 Å and 1600 Å in hydrogen-dominated (DA) white dwarfs cooler than 20,000 K and 13,500 K, respectively (Greenstein & Oke 1979; Wegner 1982). Subsequently, these features were explained by Koester et al. (1985) and Nelan & Wegner (1985) as Ly α satellite lines from collisions among H-H (1600 Å) and H-H⁺ (1400 Å). These quasi-molecular absorption lines help to constrain stellar temperature and surface gravity for DA white dwarfs (Allard & Koester 1992). G29-38, GD 133 and GD 31, the targets described in this letter, all show these quasi-molecular absorption features when observed with the *IUE* [Holm et al. (1985); Kepler & Nelan (1993), *IUE* archive]. Here, we report first detections of true molecular hydrogen in these three white dwarfs, by employing the Cosmic Origins Spectrograph (COS) on the *Hubble Space Telescope (HST)*. These three stellar atmospheres are among the hottest stellar environments where photospheric molecular hydrogen has ever been detected.

^aDepartment of Physics and Astronomy, University of California, Los Angeles CA 90095-1562; sxu@astro.ucla.edu, jura@astro.ucla.edu, kleinb@astro.ucla.edu, ben@astro.ucla.edu

^bInstitut für Theoretische Physik und Astrophysik, University of Kiel, 24098 Kiel, Germany; koester@astrophysik.uni-kiel.de

2. DATA

G29-38 and GD 133 were observed as part of program 12290 during *HST* cycle 18, which focuses on using externally polluted white dwarfs to assess the volatile abundances of accreted extrasolar planetesimals [see Jura (2003); Zuckerman et al. (2007); Klein et al. (2010); Dufour et al. (2012); Jura et al. (2012); Gänsicke et al. (2012) and references within]. G29-38 and GD 133 were chosen because they show a high degree of atmospheric pollution from optical studies (Koester et al. 1997, 2005) and display excess infrared radiation (Zuckerman & Becklin 1987; Reach et al. 2005, 2009; Jura et al. 2007). As part of our program to study Hyades white dwarfs (Zuckerman et al. 2013), ultraviolet data for GD 31 were retrieved from the *HST* archive of the SNAPSHOT program 12169 (PI: B. Gänsicke).

For G29-38 and GD 133, the COS set-up was similar to that employed for GD 40 and G241-6, as previously reported in Jura et al. (2012). The G130M grating was used with central wavelength 1300 Å and wavelength coverage of 1142 -1288 Å (strip B) and 1298 -1443 Å (strip A). The spectral resolution was $\sim 20,000$. Total exposure times, from combining 4 separate exposures for G29-38 and 5 for GD 133, were 9032 sec and 13,460 sec, respectively. The signal-to-noise ratio is at least 8 for strip B and 15 for strip A for both stars. The raw data were processed under the pipeline CALCOS 2.18.5. Because G29-38 is a ZZ Ceti star with multiple pulsation modes (Thompson et al. 2008), which lead to considerable changes in flux levels and continuum shape in each individual exposure, CALCOS processing cannot fully correct for these factors. Instead, we fitted the continuum of each CALCOS-extracted spectrum with a low-order spline3 polynomial and combined the normalized spectra with IRAF. We did not find any noticeable differences in line strength in each exposure. GD 133 is also a ZZ Ceti but the pulsation amplitude is much lower (Silvotti et al. 2006) and we simply adopt the pipeline reduced spectra. For GD 31, the G130M configuration has a central wavelength of 1291 Å, as described in Gänsicke et al. (2012). The total exposure time was 1200 sec and the signal-to-noise ratio is ~ 7 for strip A. We also used the output from the CALCOS pipeline for GD 31.

Apart from the absorption lines from heavy elements in G29-38 and GD 133, which will be discussed in Xu et al. (2013), we see numerous quasi-periodic features, as illustrated in Figure 1. They are ubiquitous between 1310 Å and 1443 Å, almost the entire strip A. Clearly, these features are real and not instrumental artifacts, such as fixed pattern noise, for the following reasons. Unlike GD 40 and G241-6 (Jura et al. 2012), two other white dwarfs observed in the same program with the same instrumental set-up, these features were only present in the spectra of G29-38 and GD 133. Furthermore, they are at the same wavelength in each separate exposure. Although initially puzzled, after comparing with the ultraviolet spectrum of the Sun (Sandlin et al. 1986), we realized the absorption wavelengths exactly

match those of molecular hydrogen. All the recognizable features correspond to Lyman band transitions from $\nu'' = 2, 3, 4, 5$ to $\nu' = 0$ and Werner band transitions from $\nu'' = 2, 3$ to $\nu' = 0$ (Abgrall et al. 1993a,b). It turns out that we have accidentally found H_2 in white dwarf atmospheres! We present the strongest Lyman band H_2 lines in Table 1; they are all appreciably stronger than the Werner bands in our observed wavelength interval.

We serendipitously identified molecular hydrogen in a third star, GD 31, which may be a high-mass escaping member of the Hyades cluster (Zuckerman et al. 2013). The data are noisier but clearly four absorption features are seen; these correspond to the strongest H_2 Lyman band lines and their blends in G29-38, at the correct wavelengths, as presented in Table 1 and Figure 1.

3. DISCUSSION

According to the Saha equation, molecular hydrogen is most concentrated in low temperature, high density environments. Previously, ro-vibrational lines from H_2 have been detected in cool stellar atmospheres in the infrared (Spinrad 1964) and in the Sun’s ultraviolet emission spectrum (Jordan et al. 1978; Sandlin et al. 1986). Our ultraviolet detection of photospheric H_2 introduces a new aspect to stellar physics. With stellar parameters of $T_* = 11,820$ K, $\log g = 8.40$ for G29-38 (Xu et al. 2013) and $T_* = 12,121$ K, $\log g = 8.005$ for GD 133 (Koester et al. 2009), we computed white dwarf model atmospheres (Koester 2010) and calculated the number density of molecular hydrogen relative to atomic hydrogen, $n(\text{H}_2)/n(\text{H})$, as shown in Figure 2. At maximum, molecular hydrogen is still $10^{-4.7}$ and $10^{-5.1}$ less than the amount of atomic hydrogen in G29-38 and GD 133, respectively. These computed ratios are comparable to, but at the higher end of the concentration of trace elements in heavily polluted white dwarfs (Jura et al. 2012). Because molecular hydrogen is distributed over a large number of ro-vibrational levels, each individual line is relatively weak. As discussed in Zuckerman et al. (2013), H_2 is used to resolve a major temperature puzzle for GD 31. Due to its high gravity, the equivalent widths (EWs) of 4 detected H_2 lines in GD 31 ($T = 13,700$ K, $\log g = 8.67$) are comparable to those in GD 133; there is a substantial amount of molecular hydrogen in the atmosphere of GD 31.

As shown in Figure 1, we computed the model spectra for G29-38 and GD 133 following Koester (2010) with all the line data obtained from the Kurucz webpage¹ (Kurucz 1995) and the H_2 partition function from Irwin (1981). In a statistical sense, the model well represents the data and reproduces most molecular hydrogen features. However, the fit to

¹<http://kurucz.harvard.edu/linelists.html>

individual lines is rather poor due to the lack of accurate broadening parameters. The Z Astrophysical Plasma Properties (ZAPP) Collaboration is actively involved in creating white dwarf photospheres in the lab and determining line broadening parameters (Falcon et al. 2012). Our understanding of the COS ultraviolet observations can be substantially improved with accurate physical parameters for the H₂ lines.

Another aspect of this discovery is that by constraining the abundance of the HD molecule, we can place a limit on the D/H ratio. It is generally believed that all deuterium is primordial from the Big Bang nucleosynthesis and destroyed in stellar interiors (Epstein et al. 1976). Any amount, if present, in the white dwarf atmosphere must come from some external source, likely relic planetesimals. The values are not very constraining for the targets presented here. But if cooler stars can be observed with COS with a sufficiently high signal-to-noise ratio, then more meaningful upper limits or actual detections of the HD molecule in white dwarf atmospheres may be anticipated.

In white dwarfs cooler than 12,000 K, H₂ is present but usually there is not enough ultraviolet flux to make observations in a time-efficient manner. The environment in hotter stars is typically more hostile for molecular hydrogen but high pressure may still enable detection of H₂.

4. CONCLUSIONS

With the *HST*, molecular hydrogen was detected for the first time in white dwarf atmospheres. The three stars, G29-38, GD 133 and GD 31, have temperatures between 11,800 K and 13,700 K. H₂ can be used as an independent constraint to white dwarf atmospheric conditions. This opens a door to many future explorations.

Support for program # 12290 was provided by NASA through a grant from the Space Telescope Science Institute, which is operated by the Association of Universities for Research in Astronomy, Inc., under NASA contract NAS 5-26555. We also utilized observations obtained [from the Data Archive] at the Space Telescope Science Institute, which is operated by the Association of Universities for Research in Astronomy, Inc., under NASA contract NAS 5-26555. These observations are associated with program # 12169. This work also has been partly supported by NSF grants to UCLA to study polluted white dwarfs.

REFERENCES

- Abgrall, H., Roueff, E., Launay, F., Roncin, J. Y., & Subtil, J. L. 1993a, *A&AS*, 101, 273
- . 1993b, *A&AS*, 101, 323
- Allard, N. F. & Koester, D. 1992, *A&A*, 258, 464
- Dufour, P., Kilic, M., Fontaine, G., Bergeron, P., Melis, C., & Bochanski, J. 2012, *ApJ*, 749, 6
- Epstein, R. I., Lattimer, J. M., & Schramm, D. N. 1976, *Nature*, 263, 198
- Falcon, R. E., Rochau, G. A., Bailey, J. E., Ellis, J. L., Carlson, A. L., Gomez, T. A., Montgomery, M. H., Winget, D. E., Chen, E. Y., Gomez, M. R., & Nash, T. J. 2012, *astro-ph 1210.7197*
- Gänsicke, B. T., Koester, D., Farihi, J., Girven, J., Parsons, S. G., & Breedt, E. 2012, *MNRAS*, 424, 333
- Greenstein, J. L. & Oke, J. B. 1979, *ApJ*, 229, L141
- Holm, A. V., Panek, R. J., Schiffer, III, F. H., Bond, H. E., Kemper, E., & Grauer, A. D. 1985, *ApJ*, 289, 774
- Irwin, A. W. 1981, *ApJS*, 45, 621
- Jordan, C., Brueckner, G. E., Bartoe, J.-D. F., Sandlin, G. D., & Vanhoosier, M. E. 1978, *ApJ*, 226, 687
- Jura, M. 2003, *ApJ*, 584, L91
- Jura, M., Farihi, J., & Zuckerman, B. 2007, *ApJ*, 663, 1285
- Jura, M., Xu, S., Klein, B., Koester, D., & Zuckerman, B. 2012, *ApJ*, 750, 69
- Kepler, S. O. & Nelan, E. P. 1993, *AJ*, 105, 608
- Klein, B., Jura, M., Koester, D., Zuckerman, B., & Melis, C. 2010, *ApJ*, 709, 950
- Koester, D. 2010, *Mem. Soc. Astron. Italiana*, 81, 921
- Koester, D., Provencal, J., & Shipman, H. L. 1997, *A&A*, 320, L57
- Koester, D., Rollenhagen, K., Napiwotzki, R., Voss, B., Christlieb, N., Homeier, D., & Reimers, D. 2005, *A&A*, 432, 1025

- Koester, D., Voss, B., Napiwotzki, R., Christlieb, N., Homeier, D., Lisker, T., Reimers, D., & Heber, U. 2009, *A&A*, 505, 441
- Koester, D., Weidemann, V., Zeidler-K.T., E. M., & Vauclair, G. 1985, *A&A*, 142, L5
- Kurucz, R. L. 1995, in *Astronomical Society of the Pacific Conference Series*, Vol. 78, *Astrophysical Applications of Powerful New Databases*, ed. S. J. Adelman & W. L. Wiese, 205
- Meyer, D. M., Lauroesch, J. T., Sofia, U. J., Draine, B. T., & Bertoldi, F. 2001, *ApJ*, 553, L59
- Nelan, E. P. & Wegner, G. 1985, *ApJ*, 289, L31
- Reach, W. T., Kuchner, M. J., von Hippel, T., Burrows, A., Mullally, F., Kilic, M., & Winget, D. E. 2005, *ApJ*, 635, L161
- Reach, W. T., Lisse, C., von Hippel, T., & Mullally, F. 2009, *ApJ*, 693, 697
- Sandlin, G. D., Bartoe, J.-D. F., Brueckner, G. E., Tousey, R., & Vanhoosier, M. E. 1986, *ApJS*, 61, 801
- Silvotti, R., Pavlov, M., Fontaine, G., Marsh, T., & Dhillon, V. 2006, *Mem. Soc. Astron. Italiana*, 77, 486
- Spinrad, H. 1964, *ApJ*, 140, 1639
- Thompson, S. E., van Kerkwijk, M. H., & Clemens, J. C. 2008, *MNRAS*, 389, 93
- Wegner, G. 1982, *ApJ*, 261, L87
- Xu, S., Jura, M., Klein, B., Koester, D., & Zuckerman, B. 2013, in preparation
- Zuckerman, B. & Becklin, E. E. 1987, *Nature*, 330, 138
- Zuckerman, B., Klein, B., Xu, S., & Jura, M. 2013, *ApJ* submitted
- Zuckerman, B., Koester, D., Melis, C., Hansen, B. M., & Jura, M. 2007, *ApJ*, 671, 872

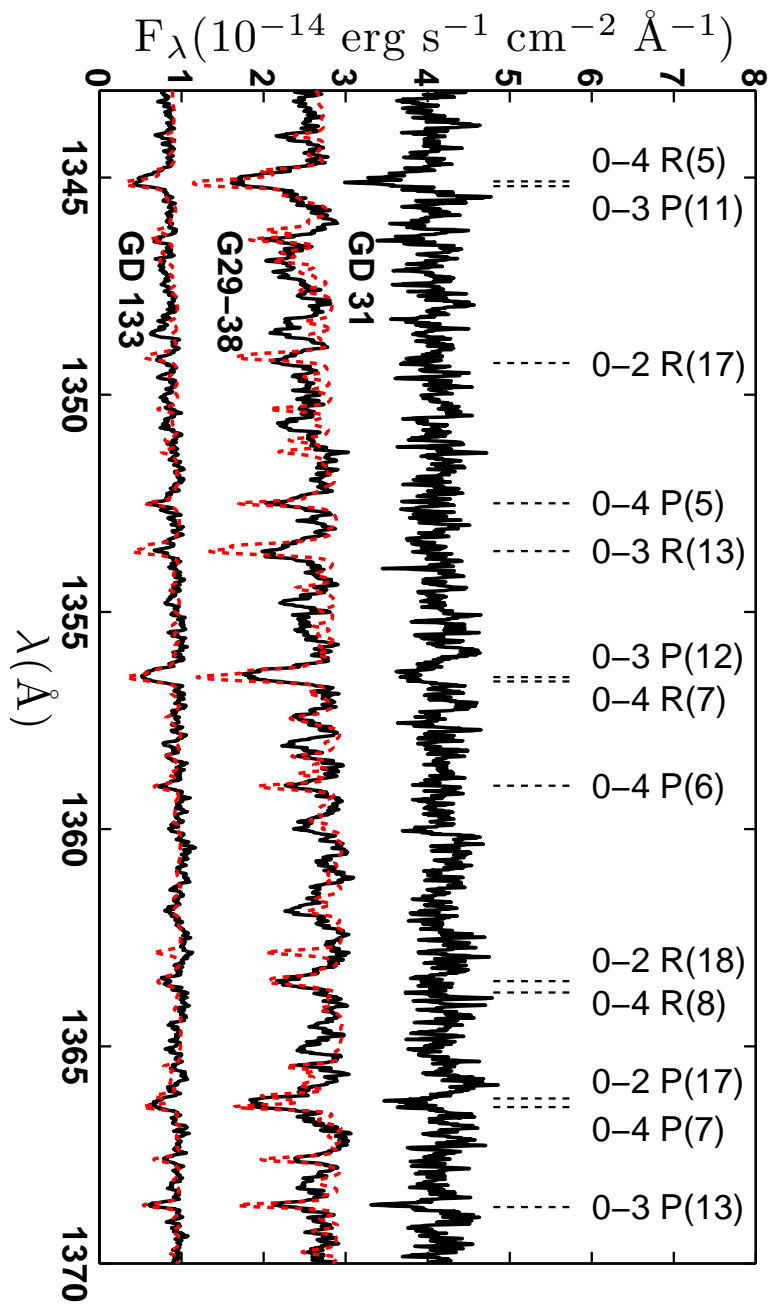


Fig 1. Portion of the Lyman band absorptions of molecular hydrogen in G29-38, GD 133 and GD 31 at the red wing of the H-H⁺ quasi-molecular feature. The spectra are smoothed with a 5 point boxcar and shifted by 39 km s⁻¹, 58 km s⁻¹ and 89 km s⁻¹ for G29-38, GD 133 and GD 31 respectively, to be in the heliocentric reference frame (Xu et al. 2013; Zuckerman et al. 2013). For clarity, the spectrum for GD 133 is offset by 0.5×10^{-14} erg s⁻¹ cm⁻² Å⁻¹ and for GD 31 by 1.5×10^{-14} erg s⁻¹ cm⁻² Å⁻¹. The red dashed lines are our computed model spectra. Statistically, the models reproduce the data but the fit to individual lines is not ideal. For G29-38 and GD 133, the entire spectrum in strip A (1298-1443 Å) shows numerous ro-vibrational lines of H₂. The strongest absorption features around 1345 Å, 1357 Å, 1366 Å and 1369 Å are also seen in GD 31.

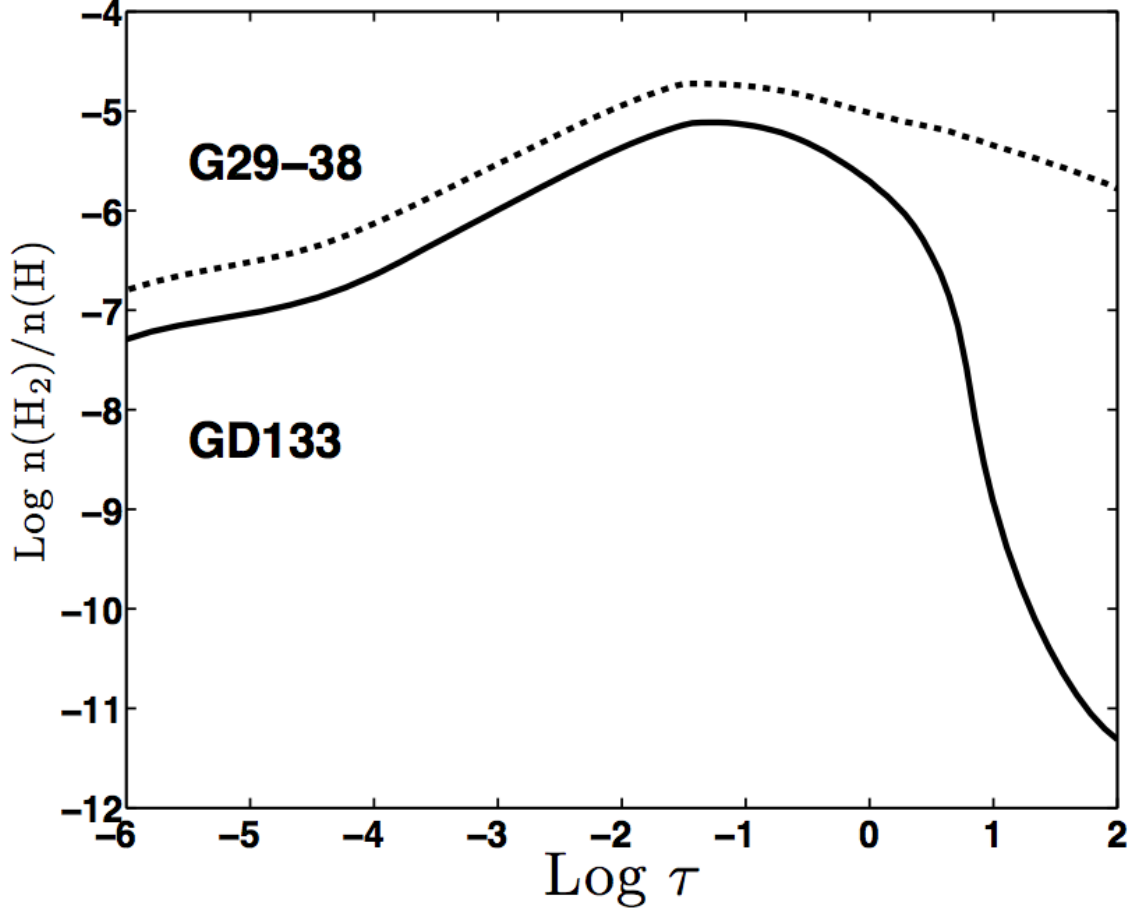


Fig 2. Ratio of number densities of molecular hydrogen compared to atomic hydrogen at different optical depths in G29-38 and GD 133. For G29-38, this ratio peaks at $\log n(\text{H}_2)/n(\text{H}) = -4.7$, where $\tau = 0.04$, $T = 9900$ K and $\rho = 3.1 \times 10^{-7} \text{ g cm}^{-3}$. For GD 133, the maximum of $\log n(\text{H}_2)/n(\text{H})$ is -5.1 , which occurs at $\tau = 0.05$, $T=10,200$ K and $\rho = 1.5 \times 10^{-7} \text{ g cm}^{-3}$.

Table 1: The Strongest Identified Lyman Band H₂ Lines

λ (cm ⁻¹) ^a	λ (Å)	Transition ^b	G29-38 EW (mÅ)	GD 133 EW (mÅ)	GD 31 EW (mÅ)
74344.49	1345.1	0-4 R(5)	170 ^c	107 ^c	87 ^c
74339.87	1345.2	0-3 P(11)	170 ^c	107 ^c	87 ^c
73936.94	1352.5	0-4 P(5)	76	66	...
73719.80	1356.5	0-4 R(7)	121 ^c	103 ^c	63 ^c
73714.96	1356.6	0-3 P(12)	121 ^c	103 ^c	63 ^c
73185.32	1366.4	0-4 P(7)	180	70	59
73064.05	1368.7	0-3 P(13)	45	35	35
71225.99	1404.0	0-4 P(11)	76	45	...
71187.04	1404.8	0-5 R(5)	97	83	...
70992.76	1408.6	0-3 P(16)	112 ^c	90 ^c	...
70889.48	1410.6	0-4 R(13)	112 ^c	90 ^c	...
70076.46	1427.0	0-4 P(13)	75	53	...

^a From Abgrall et al. (1993a).

^b We follow the notational conventions in Meyer et al. (2001).

^c This line is blended and the reported number is the total EW for both lines together.

Note. For G29-38 and GD 133, the EW uncertainty is dominated by the choice of continuum interval because the whole region shows numerous H₂ lines and there is no clean continuum as shown in Figure 1. Typically, the EW uncertainty is within 10%. For GD 31, the data are much noisier and the EW uncertainty is typically 25 %.